Metabolism Clinical and Experimental 100 (2019) 153958

Contents lists available at ScienceDirect

Metabolism Clinical and Experimental

journal homepage: www.metabolismjournal.com

Transgenic expression of the positive selected human *GLUD2* gene improves *in vivo* glucose homeostasis by regulating basic insulin secretion☆

Zoe Petraki [a], Stavros Droubogiannis [a], Konstantina Mylonaki [a], Gregory Chlouverakis [b], Andreas Plaitakis [a], Cleanthe Spanaki [a,*]

[a] Department of Neurology, School of Medicine, University of Crete, Voutes Place, 71500 Heraklion, Crete, Greece
[b] Department of Social Medicine, Biostatistics Lab, School of Medicine, University of Crete, Voutes Place, 71500 Heraklion, Crete, Greece

ARTICLE INFO

Article history:
Received 9 April 2019
Accepted 4 August 2019

Keywords:
GLUD2 transgenic mice
hGDH2
Expression
Glucose homeostasis
Body weight
Metabolism

ABSTRACT

Glutamate dehydrogenase 1 (GDH1) contributes to glucose-stimulated insulin secretion in murine β-cells, but not to basic insulin release. The implications of these findings for human biology are unclear as humans have two GDH-specific enzymes: hGDH1 (*GLUD1*-encoded) and hGDH2 (*GLUD2*-encoded), a novel enzyme that is highly activated by ADP and L-leucine. Here we studied *in vivo* glucose homeostasis in transgenic (Tg) mice generated by inserting the *GLUD2* gene and its putative regulatory elements into their genome. Using specific antibodies, we observed that hGDH2 was co-expressed with the endogenous murine GDH1 in pancreatic β-cells of Tg mice. Fasting blood glucose (FBG) levels were lower and of a narrower range in Tg (95% CI: 90.6–96.8 mg/dl; N = 26) than in Wt mice (95% CI: 136.2–151.4 mg/dl; N = 23; $p < 0.0001$), closely resembling those of healthy humans. *GLUD2* also protected the host mouse from developing diabetes with advancing age. Tg animals maintained 2.6-fold higher fasting serum insulin levels (mean ± SD: 1.63 ± 0.15 ng/ml; N = 12) than Wt mice (0.63 ± 0.05 ng/ml; N = 12; $p < 0.0001$). Glucose loading (1 mg/g, given i.p.) induced comparable serum insulin increases in Tg and Wt mice, suggesting no significant *GLUD2* effect on glucose-stimulated insulin release. L-leucine (0.25 mg/g given orally) induced a 2-fold increase in the serum insulin of the Wt mice, implying significant activation of the endogenous GDH1. However, L-leucine had little effect on the high insulin levels of the Tg mice, suggesting that, under the high ADP levels that prevail in β-cells in the fasting state, glutamate flux through hGDH2 is close to maximal. Hence, the present data, showing that *GLUD2* expression in Tg mice improves *in vivo* glucose homeostasis by boosting fasting serum insulin levels, suggest that evolutionary adaptation of hGDH2 has enabled humans to achieve narrow-range euglycemia by regulating glutamate-mediated basal insulin secretion.

1. Introduction

Glutamate dehydrogenase (GDH) (E.C. 1.4.1.3) catalyzes the reversible conversion of glutamate to α-ketoglutarate and ammonia while reducing $NAD(P)^+$ to NAD(P)H [1]. It occurs in all forms of life with most mammalian species possessing the single *Glud1* gene (*GLUD1* in the human) that encodes the evolutionary conserved GDH1 enzyme [2,3]. GDH1 is subject to strong allosteric regulation with structurally diverse compounds shown to influence its velocity [3]. Of the endogenous effectors, ADP and GTP serve as the main positive and negative modulators [3–5], with GTP interacting with GDH1 with >100-fold higher affinity (IC_{50} = 0.1–0.2 μM) than ADP (SC_{50} = 18.0 μM) [5,6]. The high sensitivity of GDH1 to GTP inhibition represents a fundamental enzyme property that largely determines glutamate flux through this pathway [3].

While GDH1 is housekeeping, its expression levels and cellular distribution are highly heterogeneous in mammalian tissues [7,8]. In most of these tissues, the direction of GDH1 reaction is towards glutamate oxidation, generating α-ketoglutarate that enters the TCA cycle leading to ATP production [3,9]. There is evidence that specialized mammalian cells utilize the GDH-catalyzed reaction to accomplish some of their unique functions [10]. In pancreatic β-cells, in particular,

Abbreviations: BAC, bacterial artificial chromosome; EDTA, ethylenediaminetetraacetic acid; FITC, fluorescein isothiocyanate; GFAP, glial fibrillary acidic protein; hGDH1, human glutamate dehydrogenase isoenzyme; hGDH2, human glutamate dehydrogenase isoenzyme 2; IF, immunofluorescence; mGDH1, mouse glutamate dehydrogenase 1; Tg, transgenic; Wt, wild-type; WB, Western blot; TCA, tricarboxylic acid cycle.

☆ This work was supported by the European Union (European Social Fund-ESF) and Greek national funds through the Operational Program "Education and Lifelong Learning" of the National Strategic Reference Framework (NSRF) - Research Funding Program: THALIS-UOA, Title "Mechanisms of pathogenesis of Parkinson's disease" (Grant Code 70/3/11679).

* Corresponding author at: Department of Neurology, School of Medicine, University of Crete, Voutes Place, 71500 Heraklion, Crete, Greece.
E-mail address: kspanaki@uoc.gr (C. Spanaki).

https://doi.org/10.1016/j.metabol.2019.153958
0026-0495/

glutamate oxidation *via* GDH1 leads to the synthesis of ATP that serves as a signal for insulin secretion [9,11,12]. Sener and Malaise [12] originally showed that L-leucine and its non-metabolized analogue BCH promote insulin release through allosteric activation of GDH1. More recent observations on mice with selective β-cell deletion of the *Glud1* gene revealed that GDH1 is essential for the full development of (glucose-stimulated) insulin secretory response, not required for glucose homeostasis under normo-caloric conditions [11].

In addition to *GLUD1*, humans have acquired *via* a recent duplication event (retro-position of *GLUD1* to the X chromosome) a novel *GLUD2* gene that encodes hGDH2 [13]. The novel gene evolved under positive Darwinian selection [14,15] indicative of adaptive DNA sequence evolution. It acquired 15 evolutionary amino acid replacements that equipped hGDH2 with unique properties [13–15]. Specifically, evolutionary replacement of Gly456 by Ala conferred resistance to GTP inhibition [16], a major functional adaptation that permits enhanced catalytic activity under conditions inhibitory to its ancestor hGDH1. Instead, hGDH2 activity is regulated *via* distinct molecular mechanisms conferred by additional evolutionary amino acid substitutions with the Arg443Ser change being the dominant player [17]. For this, hGDH2 drastically downregulates its basal activity (to 4–6% of maximal), while remaining remarkably responsive to activation by ADP (by 2500% at 1.0 mM) and L-leucine (by 1358% at 10 mM) [18]. As a result, hGDH2 has become dependent on ADP and/or Leucine for its catalysis [19]. In addition, hGDH2 shows a distinct tissue expression pattern in human tissues, including the brain, kidney, testis and steroid producing organs [10].

To better understand the role of hGDH2 in human biology, we recently generated transgenic mice expressing hGDH2 by inserting a human DNA segment containing the *GLUD2* gene and its regulatory elements into their genome [20]. Study of the *GLUD2* Tg mice brain, using double IF and confocal microscopy, revealed a hGDH2 cellular expression pattern similar to that observed in human brain [10,20]. These observations provided credence to the hypothesis that, by finding a suitable promoter in the X chromosome, the duplicated *GLUD2* gene diversified its roles in human tissues [20].

In light of these considerations, we explored here hGDH2 expression in non-neural organs (including pancreatic tissue) of Tg mice and the effect of the *GLUD2* gene on glucose homeostasis. Results revealed that hGDH2 is co-expressed with the endogenous GDH1 in pancreatic parenchyma, where it localizes to insulin-expressing cells of pancreatic islets. This hGDH2 expression "humanized" the blood glucose levels of the host by boosting fasting state serum insulin concentrations. Detailed results and the potential implications of these findings in human biology are presented below.

2. Material/methods

2.1. Reagents

The anti-hGDH1 and anti-hGDH2 specific antibodies were obtained as previously described [8,22] and used in dilutions 1:5000 and 1:2000 respectively. A mouse anti-insulin antibody (Thermo Scientific Cat.#MS-1379-P0;1:200), a goat anti-mouse secondary antibody conjugated to Alexa–Fluor 555 (Life Technologies/Thermo Fisher Scientific, A21422, 1:200), a biotinylated anti-rabbit IgG (Vector Laboratories Cat.BA-1000; 1:200) and streptavidin/FITC (Dako Code No. F 0422; 1:800) were used. Food pellets were from Mucedola 4RF21-GLP and sucralose from Splenda. Glucose was measured by a Contour NextOne glucose meter (Ascensia) and insulin with the MERCODIA Mouse Insulin ELISA10-1247-01 kit.

2.2. Generation and study of GLUD2 transgenic mice

Two independent lines of transgenic mice (Tg13 and Tg32) carrying the human *GLUD2* gene and its putative regulatory elements were constructed independently as previously described [20]. Animals were bred under specific pathogen-free conditions in the animal facility at Institute of Molecular Biology and Biotechnology (IMBB-FORTH) of Crete. The presence of the transgene was monitored by PCR from tail genomic DNA using primers specific for *GLUD2* [20]. Male Tg mice and their Wt littermates were studied.

2.3. Animal health

Animals were housed in standard cages (4 mice per cage), on a sawdust bedding, at constant temperature (23 ± 2 °C), humidity (55% ± 5%) and under a normal 12 h light/dark cycle (lights on from 7:00 to 19:00). Food and water were available ad libitum. All experimental procedures were approved by the local ethics committee for animal experimentation, meeting the governmental guidelines. Mice were sacrificed by cervical dislocation or by inhalation of an overdose of CO_2.

2.3.1. Food intake and weight comparison

Mice were weighed and food consumption was measured daily. Several physical health measures were also evaluated, including body posture, physical condition of the fur and home cage behaviors.

2.4. Enzyme assays and immunoblots

About 0.1–0.5 g of tissue (adrenals, kidney, liver, pancreas and testis) of Tg and Wt mice was homogenized (glass to glass) in 10 mM Tris-HCl, pH 7.4 buffer containing 0.1 mM EDTA, 0.5 M NaCl, 1% Triton X-100 and protease inhibitors [22]. Tissue homogenates were centrifuged (11,000 ×*g*) and the obtained extracts were used for measuring GDH activity and for immunoblot analyses. GDH activity was assayed spectrophotometrically (at 340 nm) in 50 mM triethanolamine, pH 8.0, buffer in the direction of reductive amination of α-ketoglutarate, as previously described [18]. Enzyme velocity during the first 30 s after initiation of the reaction was recorded. The amount of tissue extract loaded to immunoblots was based on its GDH activity. For WB analyses, tissue extracts were run on an 8.5% SDS-PAGE gel. Proteins were transferred on a nitrocellulose membrane and incubated with either the anti-GDH1 or the anti-hGDH2 antibody [22]. Protein bands were visualized with the use of the ChemiLucent Detection System kit (Chemicon International, Temecula, CA).

2.5. Immunofluorescence

2.5.1. Tissue slice preparation

The animals were deeply anesthetized with pentobarbital sodium (60 mg/kg, i.p.) and perfused with 30 ml PBS followed by 30 ml 4% paraformaldehyde (PFA). Tissues were removed and fixed in 4% PFA for 40 min, cryoprotected in sucrose (30% in phosphate buffer, pH 7.4), embedded in gelatin (7.5% gelatin/15% sucrose in phosphate buffer, pH 7.4) and snap frozen in isopentane.

2.5.2. Immunofluorescence

Tissue sections were cut in cryotome and fixed in acetone for 8 min. Non-specific binding sites were blocked at RT for 40 min in 5% BSA in 0.5% Triton x-100 PBS and then incubated at 4 °C for 18 h with the rabbit primary antibodies (specific for either hGDH1 or hGDH2) and with the mouse primary antibody for insulin. Tissue slides were washed 3 times in PBS and incubated with fluorescence-labeled secondary antibodies, either biotinylated goat anti-rabbit followed by Streptavidin FITC or goat anti-mouse Alexa Fluor 555. Nuclei were visualized with TOPRO. In the negative control experiments, the primary antibodies were omitted and every other step was performed as in the experimental group. For IF studies in paraffin embedded formalin fixed tissue, the slide-mounted sections were baked for 10 min at 60 °C, deparaffinized with two xylene washes, rehydrated through a series of graded alcohol washes, rinsed in water and washed with PBS (0.1 M, pH 7.4) containing 0.01% Tween 20. Heat–induced antigen retrieval was performed in a steamer using a Target Retrieval Solution (DAKO, S1700). Visualization

was performed in a confocal microscope (TCS SP2; Leica; objective 20X, numerical aperture 0.70, pinhole 1 airy unit).

2.5.3. β-Cell mass and pancreatic insulin content

Immunostaining for insulin was performed as described above. Images were collected at ×4 or ×40 magnifications. Insulin stained area, as a percentage of the whole pancreatic area, was multiplied by pancreas weight to calculate β-cell mass. Islet area was calculated by dividing the insulin-positive area by the islet number for each tissue section. β-Cell cross-sectional area was calculated by dividing the insulin-positive area by the number of β-cell nuclei. β-Cell density was determined by dividing the number of β-cell nuclei by total pancreatic area.

2.6. Blood glucose and insulin determination

For determining blood glucose levels, the facial vein was punctured with a 31G needle and blood drops were collected in a tube. Insulin concentrations were determined in the serum. Glucose tolerance tests (GTT) were performed by administering i.p. 1 mg/g of body weight of glucose solution after fasting for 6 or 12 h. Blood samples were collected from the tail tip at 0, 30, 60, 90 and 120 min after glucose administration. Tg and Wt mice were studied in parallel. Insulin tolerance test was performed by administering i.p. 1 IU/kg body weight of human insulin (rDNA) (Actrapid 100 IU/ml, Novo Nordisk), following a 5 h-long morning fasting period (light cycle). Glucose concentration was monitored every 15 min for up to 2 h (120 min). Three-month-old mice of similar body weight were selected for this study. Ten Tg and ten Wt mice were studied in parallel.

2.6.1. Oral leucine loading

Mice were fed L-leucine *via* a non-invasive voluntary method. For this, L-leucine powder was incorporated into an artificially sweetened jelly containing sucralose, a sucrose-derived non-caloric sweetener that does not stimulate insulin release and does not interfere with our measurements. The jelly was prepared using 40 μl of 20% w/v sucralose solution in drinking H_2O with 60 μl of 14% w/v gelatin in 20% sucralose solution. The mixture was poured into a mold and let it set at 4 °C. L-leucine was then added to the jelly in an amount that provided 0.25 mg/g body weight. To overcome neophobia, a training period preceded the experiments, during which mice were exposed to the sweetened jelly without leucine. Once the animals were able to eat the jelly, single housed mice were fed the L-leucine-containing jelly after overnight fasting. A vehicle jelly preparation without L-leucine was used as control. Blood samples were collected at 0, 30 and 60 min after L-leucine administration for glucose and insulin determination.

2.6.2. Statistical analysis

Summary descriptive statistics are given as mean ± SD. Independent samples *t*-tests were used to compare continuous variables between the Tg and Wt groups. One-way ANOVA was used to evaluate differences between the three mice groups (Tg13, Tg32, Wt). Repeated Measures ANOVA was used to assess time, group and time-group interaction effects of continuous variables measured at several time points. Post-hoc Bonferroni adjusted tests were used to pinpoint differences. Linear regression analyses of glucose levels with the age of the animals were performed. *p*-Values <5% was the criterion for significance. All analyses were performed using the IBM-SPSS 25. Graphical representations were done using the GraphPad Prism 6.

3. Results

3.1. Health measures of GLUD2 transgenic mice

Two lines of transgenic mice (Tg13 and Tg32), generated independently [20], were used for these studies. The breeding rates of Tg and Wt mice were comparable, with the Tg mice passing their developmental milestones at about the same time as their wild-type littermates. Also, no differences were detected between Wt and Tg mice regarding food consumption, home cage behavior, body posture, and the physical appearance of the animals' fur. Similarly, irregular behaviors such as excessive grooming, digging, rearing, or stereotypies were not different between the two groups. Survival rates were also comparable between Tg and Wt mice.

3.2. Effect of the GLUD2 gene on tissue GDH activity

Enzyme assays, performed on tissue homogenates from Tg and Wt mice, revealed marked inter-tissue GDH differences within each group, with the highest GDH activity found in the liver and the lowest in the testis (Fig. 1). These results are consistent with the inter-tissue GDH disparities detected in several mammalian species, including the human [7,8]. A significant *GLUD2* gene effect on tissue GDH activity was detected for the testis. Thus, as shown in Fig. 1, the GDH activity of Tg mice testis (2.26 ± 0.27 μmol NADPH oxidized/mg tissue/min) was about twice as high as that of Wt testis (1.00 ± 0.14 μmol NADPH oxidized/mg tissue/min; $p = 0.0002$). As such, assaying enzyme activity proved sensitive for detecting a *GLUD2* gene effect in a tissue characterized by low endogenous GDH1 activity. In the kidney and pancreas of Tg mice, GDH activity was 25–30% higher than that of Wt mice; however, due to inter-animal variability, these differences did not reach statistical significance, although WB and IF studies revealed hGDH2 expression in Tg mice tissues (see below). In the liver, GDH activity was essentially the same in Tg and Wt mice, although WB detected hGDH2 expression in Tg liver. As our enzyme assay measures the sum of the GDH1 and hGDH2, determination of total GDH activity (as done here) lacks the sensitivity needed for detecting hGDH2 expression in tissues with relatively high levels of endogenous GDH1.

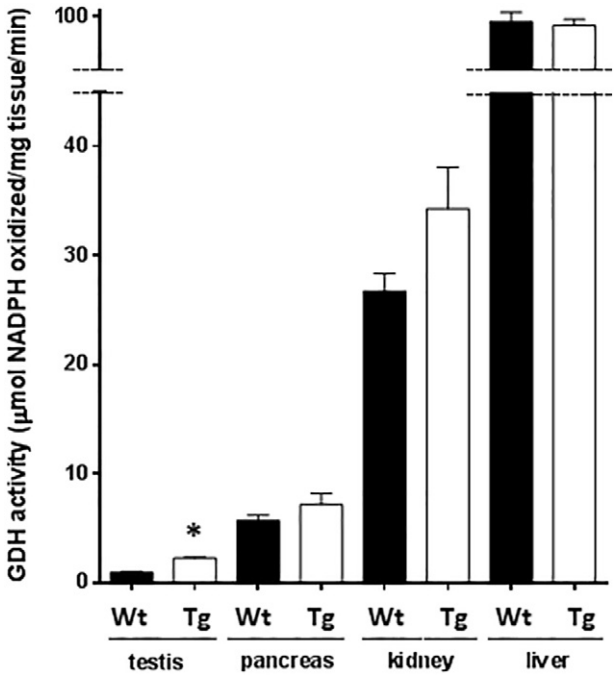

Fig. 1. Tissue GDH activity of *GLUD2* transgenic (Tg) mice and their wild type (Wt) littermates. Enzyme activity was measured in whole homogenates from the tissues shown in the figure as described in the Material/methods. Assays were performed in 50 mM, pH 8.0, triethanolamine (TRA) buffer in the presence of 1.0 mM ADP. Activities are expressed as μmol NADPH oxidized per mg wet tissue per min. Black filled and white columns represent mean values for Wt and Tg mice respectively, and bars SEM. Three wild-type (Wt) and six *GLUD2* transgenic mice (Tg) were studied. The Tg group consisted of three Tg13 and three Tg32 mice. Differences between Tg and Wt animals reached significance only for testis (*$p = 0.0002$).

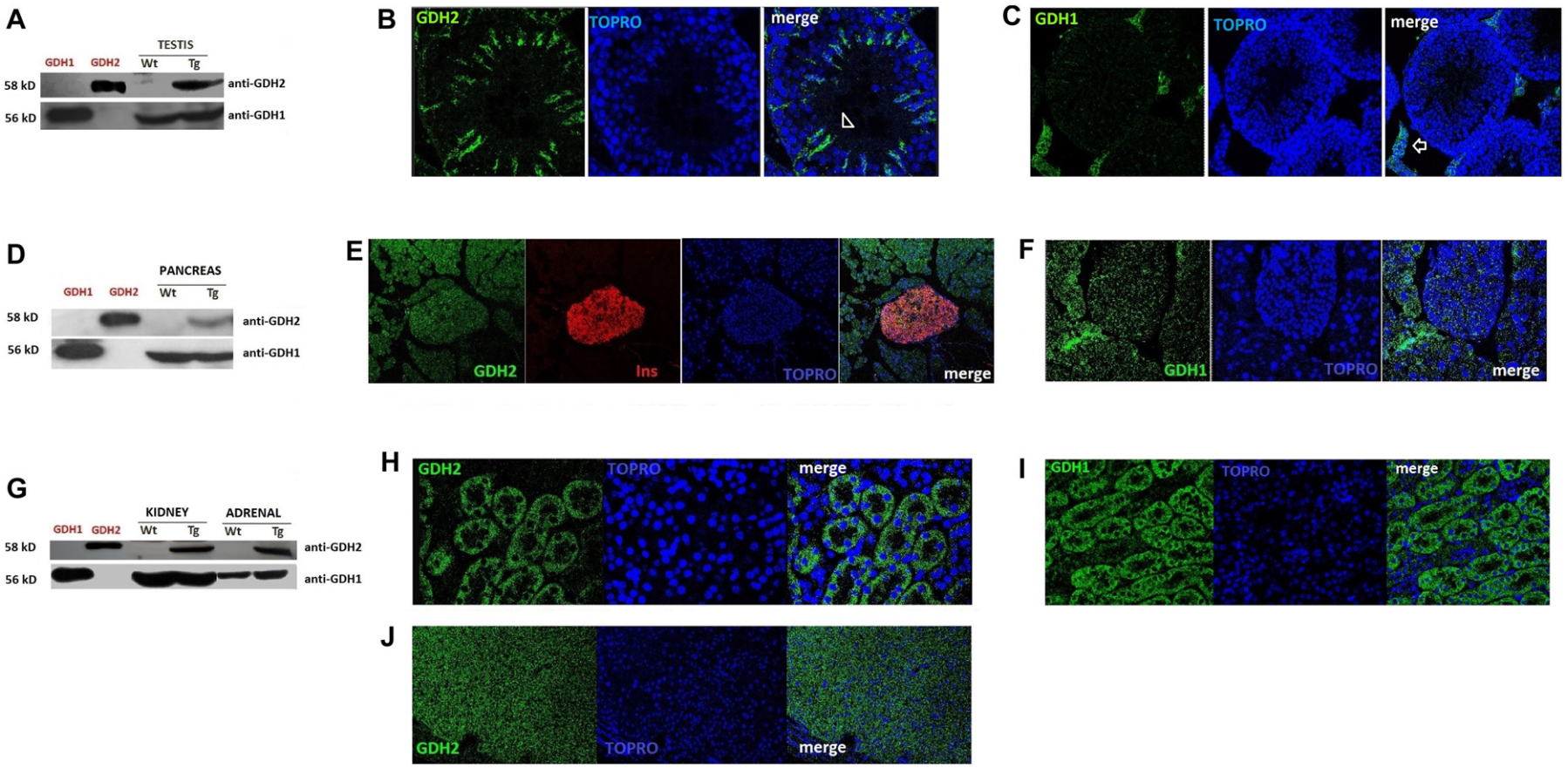

Fig. 2. hGDH2 expression in testis, pancreas, kidney and adrenals of Tg and Wt mice. A–J. Adult (6-month-old) *GLUD2* transgenic (Tg) mice and their wild-type (Wt) littermates were used for these experiments. A, D, G. Western blots were probed with either the anti-hGDH2 or the anti-hGDH1 antibody; purified recombinant hGDH1 and hGDH2 were used as controls. Tissue homogenates with comparable GDH activity (as determined by enzyme assays) were loaded into the gels. All tissues shown in this figure were from Tg32 mice. Similar results were obtained with the use of Tg13 mice. A. Immunoblots of testicular tissue extracts detected a hGDH1-postive band in Tg and Wt mice that corresponds to recombinant hGDH1 and represents the endogenous mouse-GDH1. In contrast, a hGDH2-specific band was detected in the Tg mice only, corresponding to recombinant hGDH2. B. IF on paraffin embedded fixed Tg testis using the anti-hGDH2 antibody (green). (White empty arrowhead: hGDH2-specific labelling of Sertoli cells). C. IF of paraffin embedded fixed Tg testis using the anti-hGDH1 antibody (green). (White empty arrow: GDH1-specific labelling of Leydig cells in the interstitium.) D. Immunoblots of pancreatic extracts containing similar GDH enzymatic activity from Tg and Wt mice probed with the anti-hGDH2 or the anti-GDH1 antibody. The hGDH2-specific band, detected in Tg mice only, corresponds to recombinant hGDH2, whereas the hGDH1-specific band, detected in both the Tg and Wt mice, corresponds to recombinant hGDH1. E. Double IF studies on paraffin embedded fixed pancreatic tissue using the anti-hGDH2 antibody and a mouse anti-insulin specific antibody. hGDH2-specific immunoreactivity (green) was detected in the Langerhans islets where it localizes to insulin-expressing cells (ins in red). In addition, pancreatic cells outside Langerhans islets were labeled by the hGDH2-specific antibody. F. The hGDH1-specific antibody also visualized both pancreatic islets and cells surrounding the Langerhans islets (green). G. Immunoblots of renal tissue from Tg and Wt mice using the anti-hGDH2 or the anti-GDH1 antibody. The hGDH2-specific band detected in Tg mice, corresponds to the purified recombinant hGDH2, whereas the hGDH1-specific band seen in renal tissue from both the Tg and Wt mice corresponds to the recombinant hGDH1 protein. H & I. IF studies on formalin fixed paraffin embedded renal tissue using either the anti-hGDH2 antibody (green) (H) or the anti-GDH1 antibody (green) (I). Epithelial cells lining the proximal renal tubules were stained with both antibodies. J. IF studies using formalin fixed paraffin embedded adrenals from Tg mice showing expression of hGDH2 in all layers of the adrenal cortex. Blue stain: Cell nuclei visualized with TOPRO. Tissue sections were viewed using a confocal microscope (TCS SP2; Leica). Settings used: objective 20×, numerical aperture 0.70, pinhole 1 au (airy unit) for figures C, E, H, I, J and 40× with numerical aperture 1.25 and pinhole 1 au for B. (For interpretation of the references to color in this figure legend, the reader is referred to the web version of this article.)

3.3. Western blots show expression of hGDH2 in Tg mice tissues

Two antibodies specific for either hGDH2 or hGDH1 [10] were used for WB analyses. Results revealed that the anti-hGDH1 antibody interacted with the endogenous mouse GDH1 (mGDH1) with the same affinity as with hGDH1, without recognizing the expressed hGDH2 (Fig. 2A, D, G). These results are expected as hGDH1 and mGDH1 are essentially identical, having been conserved *via* purifying selection [14]. Conversely, our anti-hGDH2 antibody recognized the expressed hGDH2 protein without interacting with the endogenous mGDH1 enzyme. In *GLUD2* Tg mice, hGDH2 was expressed in the adrenals, kidney, liver, pancreas and testis (Fig. 2). In testicular tissue, hGDH2 and mGDH1 were expressed at equal levels (Fig. 2A), whereas in other tissues hGDH2 was expressed at lower levels than the endogenous mGDH1. In addition, hGDH2 expression did not affect the endogenous mGDH1 levels in all Tg animal tissues studied, as detected with the use of the anti-hGDH1-specific antibody (Fig. 2A, D, G). No significant hGDH2 expression was identified in adipose tissue and skeletal muscle.

3.4. Cellular expression of the GLUD2 gene in Tg mice tissues

Immunofluorescence (IF) studies on testicular tissue revealed that hGDH2 was expressed in the Sertoli cells located inside the seminiferous tubules (Fig. 2B), and in the Leydig cells located in the interstitium. In contrast, mGDH1 was absent from the Sertoli cells, but was instead expressed in the Leydig cells (Fig. 2C). This expression pattern is identical to that observed in human testis where hGDH2 localizes to Sertoli cells, which lack hGDH1 [10]. Also, our observations showing that hGDH2 and mGDH1 attained in Tg testis equivalent levels are again strikingly similar to those previously reported for human testis, in which hGDH2 and hGDH1 are expressed at equal levels [10]. The unique expression of hGDH2 in Sertoli cells, as shown here, is thought to contribute to glutamate oxidation-derived lactate that is provided to sperm cells [10].

In the pancreas, double IF experiments showed that hGDH2 was expressed along with mGDH1 throughout the parenchyma, where it localized to insulin-expressing cells of pancreatic islets (Fig. 2E, F). We then tested whether transgenic expression of the human *GLUD2* gene affected the morphology or quantity of the β-cells. For this, we studied haematoxylin–eosin stained sections of pancreatic tissue as well as sections of fixed frozen pancreatic tissue immunostained with an antibody against insulin. Results revealed no significant differences between Tg and Wt mice with respect to the number or size of Langerhans islets or in the number and mass of β-cells (data not shown).

In the kidney, hGDH2 co-localized with the endogenous mGDH1 in the epithelial cells that line the proximal convolutional tubules (Fig. 2H, I), in accordance with previous observations on human renal cortex [21]. Given the ability of hGDH2 to work efficiently at relatively low pH and at GTP concentrations inhibitory to hGDH1 [18], expression of the novel enzyme in renal epithelial cells is thought to enhance glutamate deamination-derived ammoniagenesis (particularly during acidosis), thus contributing to acid-base balance [21].

In the adrenals, hGDH2 was co-expressed along with mGDH1 in all three layers of adrenal cortex that produce steroid hormones, including the zona glomerulosa (mineralocorticoid-secreting), the zona fasciculata (glucocorticoid-producing) and the zona reticularis (androgen-producing) (Fig. 2J). This cellular distribution pattern is similar to that previously observed for hGDH1 and hGDH2 in human adrenals [22]. Expression of hGDH2 in these cells is thought to provide a GTP-independent source of reducing equivalents (NADPH) needed for pregnenolone synthesis (initial step in steroidogenesis), as well as, an additional mechanism for feedback control of steroid synthesis [22].

3.5. Effect of the GLUD2 transgene on fasting glucose and insulin levels

Biochemical analyses of blood samples, obtained from young adult animals (3–6 months of age) after overnight (12-h long) fasting, revealed that blood glucose levels were significantly lower and of a narrower range in Tg mice (mean ± SD: 93.7 ± 7.6 mg/dl; 95% CI: 90.6–96.8 mg/dl; N = 26) as compared to their Wt littermates (mean ± SD: 143.8 ± 17.5 mg/dl; 95% CI: 136.2–151.4 mg/dl; N = 23; $p < 0.0001$) (Fig. 3A). As such, Tg mice had fasting blood glucose (FBG) values essentially identical to those of healthy (non-diabetic) humans. It is known that the C57BL/6J mouse strain used here is prone to diabetes, particularly with advancing age [23]. Our data indeed showed that Wt mice >12 months of age had significantly higher FBG levels (mean ± SD: 161.1 ± 24.8 mg/dl; N = 29; $p = 0.005$) than younger Wt animals (Fig. 3B). This aging effect was substantially attenuated in Tg mice (Fig. 3B). As shown in Fig. 3E, FBG levels correlated with the age (in weeks) of both Tg ($R^2 = 0.429$) and of Wt ($R^2 = 0.235$) mice. We also found that fasting for 6 h (prior to blood drawing) was associated with even higher FBG levels in aged Wt mice (192.0 ± 21.1 mg/dl; 95% CI: 176.9–207.1 mg/dl (N = 10)), with about half of these values being >200 mg/dl (considered to be pre-diabetic for C57BL/6J mouse strain) (Fig. 3D) [23]. Remarkably, *GLUD2* exerted a considerable protective effect against the propensity of the host mice to develop diabetes with aging. Thus, after fasting for 6 h, the FBG levels of Tg mice were 119.9 ± 12.8 mg/dl (95% CI: 110–130 mg/dl; N = 9; $p < 0.0001$) (Fig. 3D). Measurement of insulin concentrations in both animal groups revealed that fasting serum insulin levels were about 2.6-fold higher in Tg (mean ± SD: 1.67 ± 0.15 ng/ml; 95% CI: 1.58–1.77; N = 12; $p < 0.0001$) than in Wt mice (0.65 ± 0.06 ng/ml; 95% CI: 0.61–0.69; N = 12) (Fig. 3C). The same *GLUD2* gene effect on FBG and serum insulin levels was found in both of our Tg lines (Tg13 and Tg32) (Fig. 3A, B, C and D).

3.6. The GLUD2 gene does not affect glucose-stimulated serum insulin increase

Serum insulin levels rose robustly in Tg and Wt mice following administration of glucose (1 mg/g body weight, given i.p.) (Fig. 4A). This increase was in absolute value comparable between Wt (by 1.34 ± 0.45 ng/ml) and Tg mice (1.26 ± 0.19 ng/ml). However, because baseline insulin levels were lower in Wt mice (Fig. 4A), the glucose-stimulated serum insulin increases were proportionally greater in Wt (by 214 ± 80%) than in Tg animals (77 ± 10%). Similarly, blood glucose levels rose significantly in both animal groups after glucose administration (Fig. 4B). While this increase was in absolute value identical in Wt (by 202 ± 31 mg/dl) and in Tg mice (205 ± 18.9 mg/dl), the Wt group showed proportionally smaller blood glucose increases due to its higher FBG levels. Analysis of our data (Fig. 4A and B) using repeated measures ANOVA revealed a significant effect of genotype (Wt v/s Tg) on both serum insulin ($p < 0.001$) and glucose levels change ($p < 0.001$) following glucose administration, a finding attributed to the significantly different baseline insulin and glucose levels of the Tg and Wt animals. Our two transgenic lines, Tg13 and Tg32 behaved similarly ($p = 0.999$). A second independent experiment, performed at a different date, yielded nearly identical results for both of our Tg lines.

3.7. L-leucine loading boosts serum insulin levels in Wt mice

To evaluate glucose-independent insulin secretion, we performed L-leucine loading experiments by administering orally 0.25 mg/g body weight to Tg and Wt mice. L-leucine resulted in a robust increase in the serum insulin levels of the Wt mice (before loading 0.68 ± 0.07, after loading: 1.25 ± 0.076 ng/ml; $p < 0.0001$), but it had little effect on the high fasting insulin levels of the Tg mice (baseline: 1.71 ± 0.15,

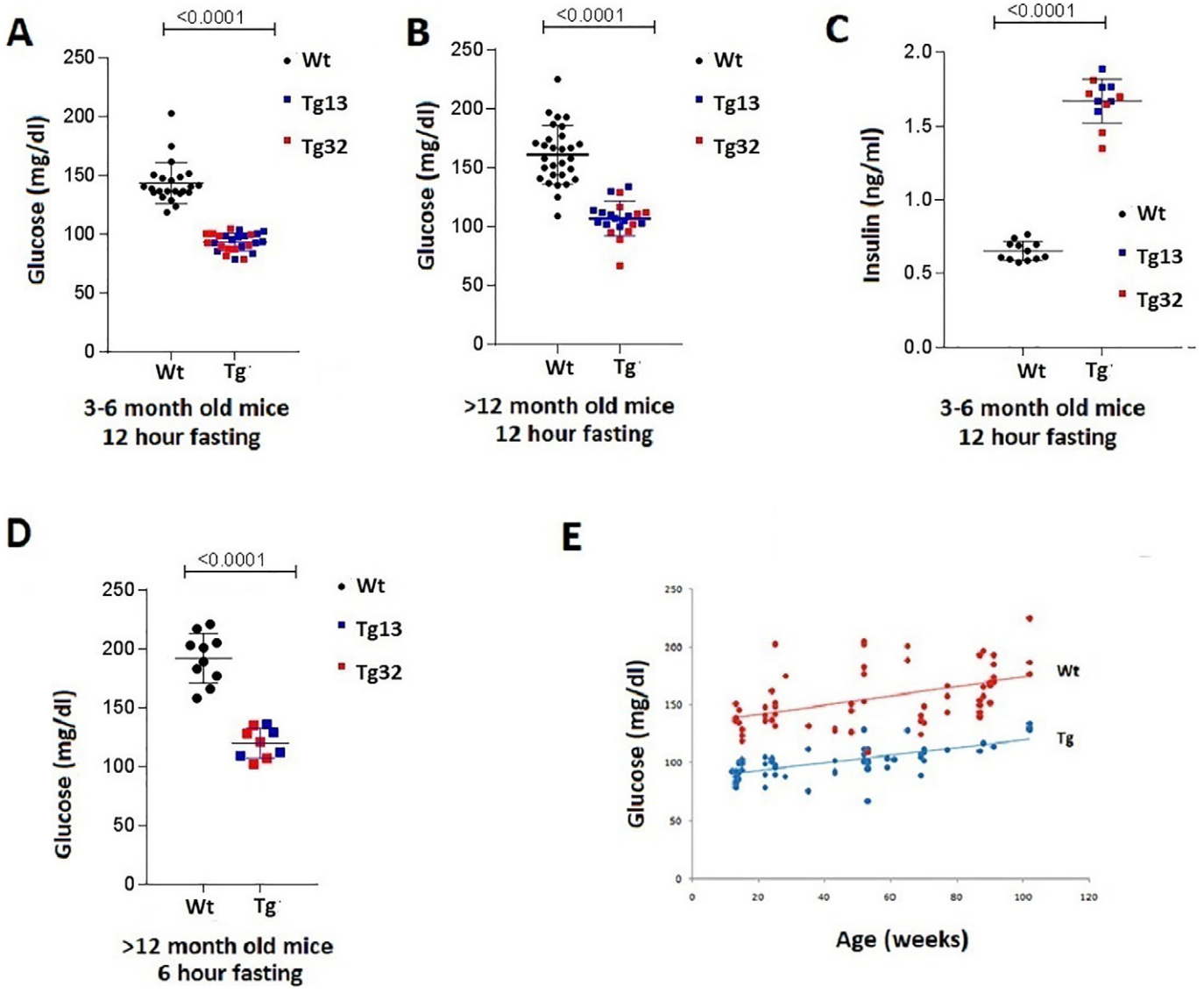

Fig. 3. Glucose homeostasis in Tg and Wt mice of different ages. A–E: Fasting blood glucose (FBG) levels of Tg and Wt mice. The age of the animals and the fasting interval (prior to blood drawing) are shown below each figure. The *p* value above the figures refers to comparison between Tg and Wt mice of the same age. A. FBG levels of young adult (3–6-month-old) mice (Wt: N = 23, Tg: N = 26; Tg32: N = 12, Tg13: N = 14). B. FBG levels of 12–24-month-old (≥12-month-old) animals (Wt: N = 29, Tg: N = 21; Tg32: N = 9, Tg13: N = 12). FBG levels were significantly higher in aged (>12-month-old) Wt mice as compared to young adult (3–6-month-old) Wt animals ($p = 0.005$). Similarly, FBG were higher in older Tg mice as compared to younger Tg animals ($p = 0.0007$). C. Blood insulin levels were obtained after overnight fasting in young adult (3–6 months of age) Wt (N = 12) and Tg mice (N = 12; Tg13: N = 6; Tg32: N = 6). D. FBG levels were obtained after a 6-hour fasting in 12–24-month-old (mean age: 15 months) Tg (N = 9, Tg32: N = 5, Tg13: N = 4) and Wt mice (N = 10). E. Correlation of glucose levels (obtained after a 12-hour fasting) with the age of the animals ($r^2 = 0.24$ for Wt and $r^2 = 0.43$ for Tg mice). Each dot represents the FBG levels of a single animal.

after loading: 1.90 ± 0.26 ng/ml; $p = 0.154$) (Fig. 4C). In addition, L-leucine loading reduced the blood glucose levels of Wt mice (baseline: 164 ± 24 mg/dl; after loading: 137 ± 24 mg/dl; N = 6), but had essentially no effect on the glucose levels of the Tg mice (baseline: 100 ± 5 md/dl; after loading: 104 ± 2; N = 6) (Fig. 4D). Analysis of our data (Fig. 4C and D) with repeated measures ANOVA revealed a significant effect of the genotype (Wt v/s Tg) on insulin and glucose changes following leucine administration ($p < 0.001$ for insulin and $p = 0.001$ for glucose) (Fig. 4C and D). Leucine differentially affected insulin and glucose levels in the two groups (repeated measures ANOVA interaction effect $p < 0.001$).

3.8. L-leucine loading improves glucose tolerance in Tg and Wt mice

To test whether L-leucine pre-treatment affects glucose handling, we administered 1 mg/g glucose (i.p.) to Wt and Tg mice half an hour after an L-leucine load (0.25 mg/g). Insulin and glucose levels were determined

Fig. 4. A & B: The *GLUD2* gene does not affect glucose-stimulated insulin release. Young adult (4-month old) Tg and Wt mice received i.p. 1.0 mg/g weight of glucose after a 12 hour-long fasting. Insulin (A) and glucose levels (B) were measured before (0 time) and 60 min after glucose administration. Compared to Wt mice, the Tg animals had, both at baseline and following glucose administration, higher insulin ($p < 0.001$) and lower blood glucose levels ($p < 0.001$). Repeated measures ANOVA suggested a significant genotype effect (Wt v/s Tg) on insulin ($p < 0.001$) and glucose changes ($p < 0.001$) following glucose administration, attributed to baseline level differences. C & D: L-leucine loading differentially affects serum insulin levels of Wt and Tg mice. Young adult (5-month old) Tg and Wt mice received orally L-leucine (0.25 mg/g of body weight) after fasting for 12 h. Serum insulin and blood glucose levels were then determined at 0 time and 60 min later. Repeated measures ANOVA revealed a significant genotype effect on insulin ($p < 0.001$) and glucose ($p = 0.001$) changes following leucine loading. E: Pre-treatment with L-leucine improves glucose handling in Tg and Wt mice-Young adult (5-month old) Tg and Wt mice received orally L-leucine (0.25 mg/g of body weight) after fasting for 12 h. Half an hour after L-leucine treatment, the animals received i.p. 1.0 mg/g weight of glucose. Serum insulin levels were measured before (0 min) and 60 min after glucose administration (E). Repeated measures ANOVA revealed a significant genotype effect on insulin changes induced by glucose administration, following leucine pre-treatment ($p < 0.001$).

1 h later. Results revealed enhanced insulin release in both Wt and Tg mice (Fig. 4E). While in absolute values, these insulin increases were comparable in the two animal groups, Wt mice again experienced greater proportional increases (4-fold) than Tg animals (2-fold). Insulin levels were somewhat higher than those obtained following glucose administration but without L-leucine pre-treatment in both groups (Fig. 4A). Blood glucose levels also increased comparably in Tg and Wt mice as shown in Fig. 5A. However, blood glucose increases were of a lesser magnitude that those found in animals not pre-treated with L-leucine. Analysis of the data presented in Fig. 4E with repeated measures ANOVA revealed a significant genotype effect (Wt v/s Tg) on insulin changes induced by glucose administration following leucine pre-treatment ($p < 0.001$).

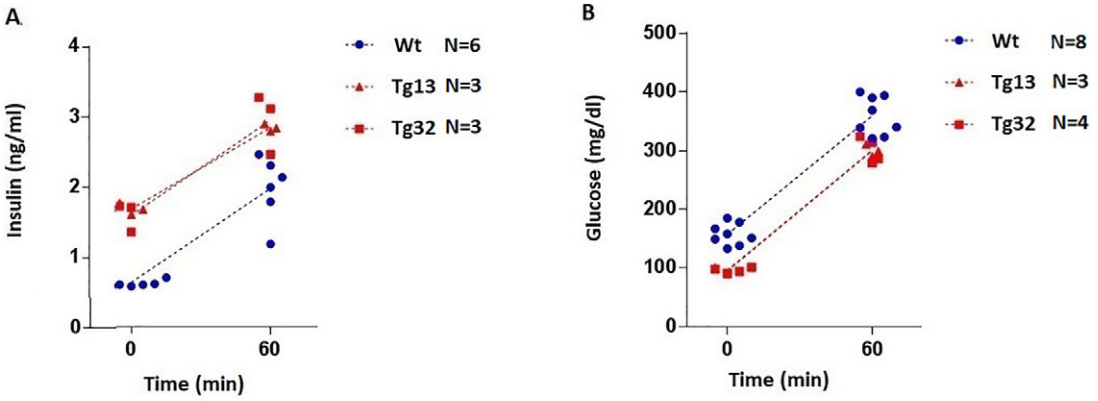

Changes in Insulin and Glucose levels after Glucose administration to Wt and Tg mice

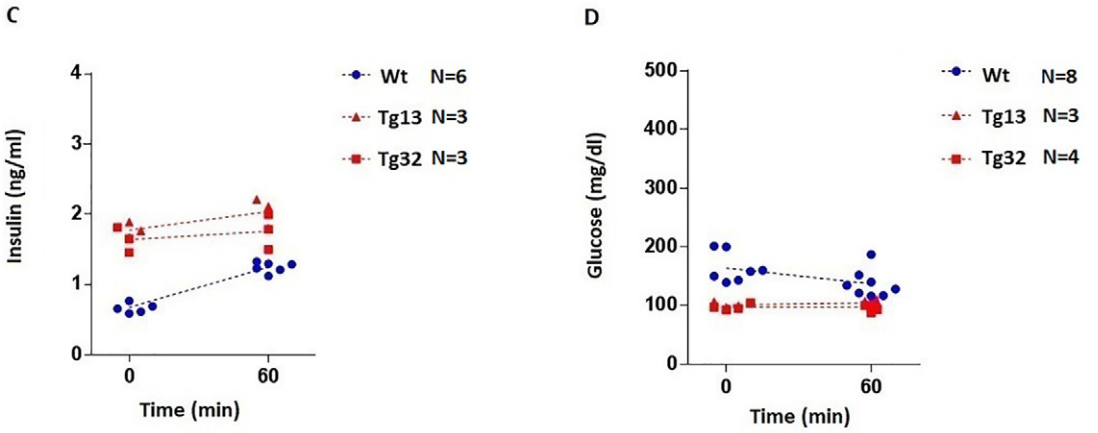

Changes in Insulin and Glucose levels after L-leucine administration to Wt and Tg mice

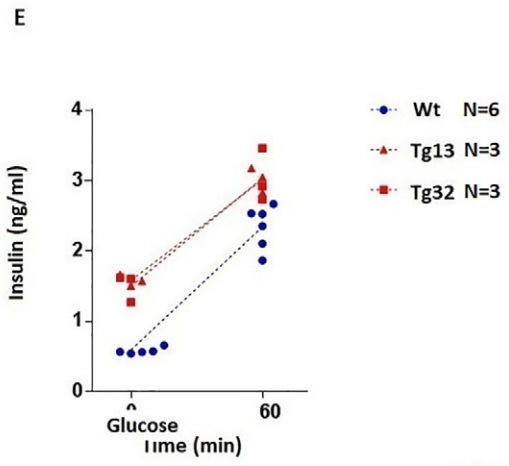

Changes in Insulin levels after Glucose administration to Wt and Tg mice pre-treated with L-leucine. Changes in Glucose levels are shown in Figure 5A

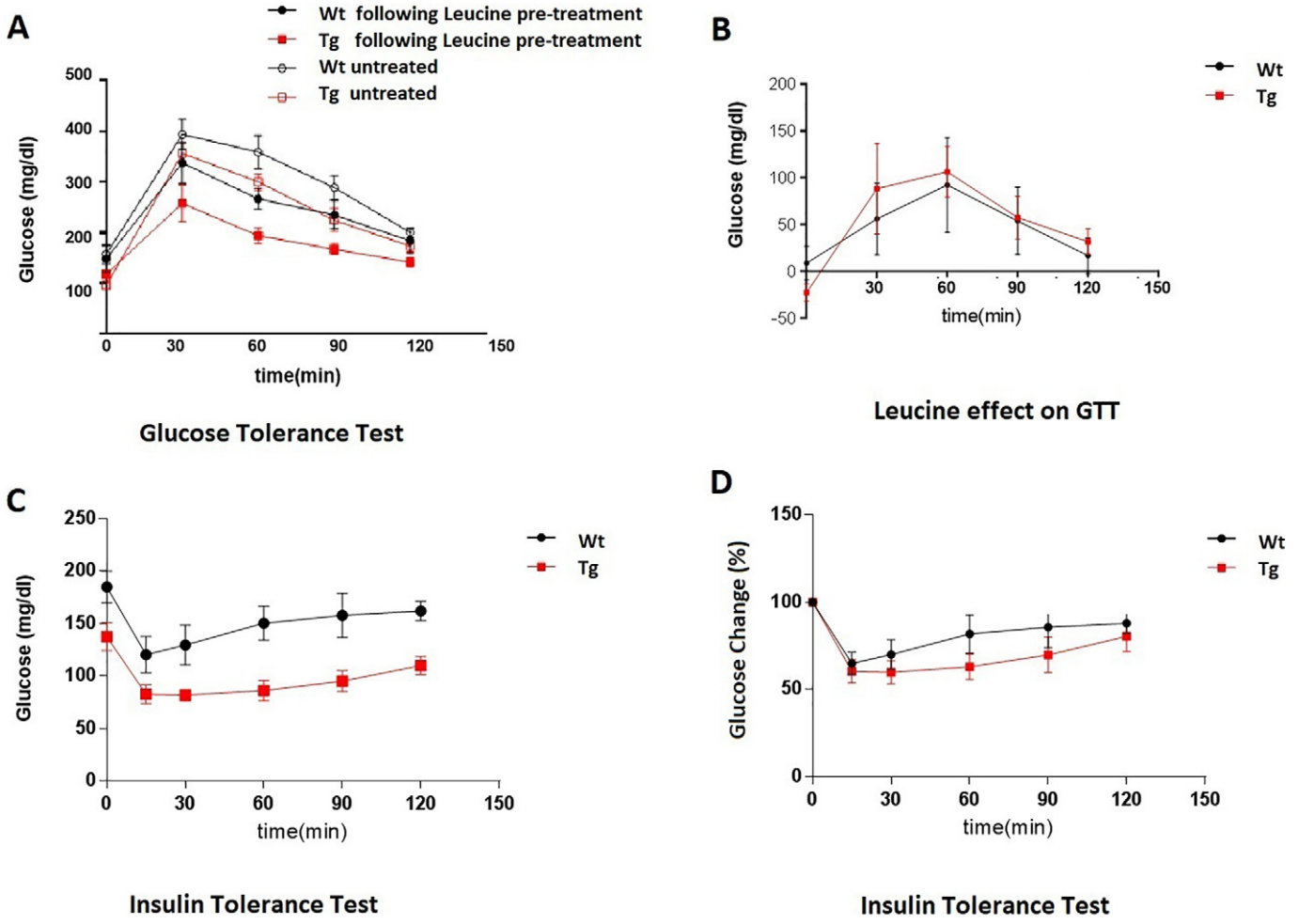

Fig. 5. A & B: L-leucine effect on the GTT curves of Tg and Wt mice. A. GTT was performed in 5-month-old Wt (N = 8) and Tg (N = 7; Tg13 = 3 and Tg 32 = 4) mice either without pre-treatment (untreated) or ½ h after administration of 0.25 mg/g of L-leucine (Leucine pre-treatment). Repeated measures ANOVA revealed a significant genotype effect ($p < 0.001$) on glucose changes over time. B. The differences in glucose levels induced by leucine pre-treatment were plotted over time. No differential effect of L-leucine on the GTT curves of Tg and Wt mice was detected ($p = 0.730$). C & D. Insulin tolerance test in Wt and Tg mice. Wt (N = 10) and Tg (N = 10; Tg13 = 5 and Tg32 = 5) mice received i.p. 1 IU/kg of insulin after a 5 h-long morning fasting period. Blood glucose levels were determined at the time points shown here. A significant genotype effect was suggested and attributed to different baseline glucose levels ($p < 0.001$). D. The changes in blood glucose levels induced by insulin administration (expressed as percentage of initial) were plotted over time. There was no differential effect of insulin on blood glucose levels in the two groups (ANOVA $p = 0.603$).

3.8.1. Glucose tolerance studies

GTTs were also performed by administering a glucose load (1 mg/g body weight, i.p.) with and without L-leucine pre-treatment (given 30 min prior to glucose administration). Tg mice showed improved glucose curves as compared to their wild type littermates in both conditions (with and without L-leucine pre-treatment). Repeated measures ANOVA analysis of the data presented in Fig. 5A suggested a significant effect of genotype (Wt v/s Tg) on blood glucose changes over time regardless of leucine pre-treatment ($p < 0.001$). On the other hand, L-leucine pre-treatment resulted in a better handling of glucose in both groups. A significant effect of leucine pre-treatment on glucose changes over time (GTT curves) was detected for both groups (ANOVA $p < 0.001$ for Wt and for Tg mice). The net changes in glucose levels during the GTT induced by L-Leucine pre-treatment were plotted over time (Fig. 5B). Results revealed that leucine pre-treatment affected similarly the GTT curves of Wt and Tg animals (repeated measures ANOVA $p = 0.730$).

3.8.2. Insulin sensitivity studies

Insulin tolerance test were also performed in young adult (3-month old) Wt (N = 10) mice and Tg (N = 10; Tg13 = 5 and Tg32 = 5) animals by administering i.p. 1 IU/kg body weight of human insulin following a 5 h morning fasting period (light cycle). Determination of blood glucose levels was done at 15, 30, 60, 90 and 120 min after insulin administration. Results revealed that glucose levels declined in both animal groups (Fig. 5C and D). Analysis of data presented in Fig. 5C with repeated measures ANOVA suggested a differential effect of genotype (Wt v/s Tg) on the insulin induced change of blood glucose levels over time ($p < 0.001$). This was attributed to the significantly different baseline glucose levels of the two groups. However, blood glucose levels decreased proportionally following insulin administration in both animal groups (Fig. 5D). Furthermore, the course of insulin-induced drop in glucose levels over time did not differ between the two groups (repeated measures ANOVA showed no significant genotype effect; $p = 0.603$). These results, revealing similar insulin tolerance tests for Wt and Tg mice, suggest that the two groups are comparably sensitive to insulin.

3.8.3. Effect of aging on food consumption and body weight

Food consumption, studied at different ages, was found to be comparable between the two experimental groups. The body weight of young adult (2-month-old) Tg and Wt mice did not differ significantly

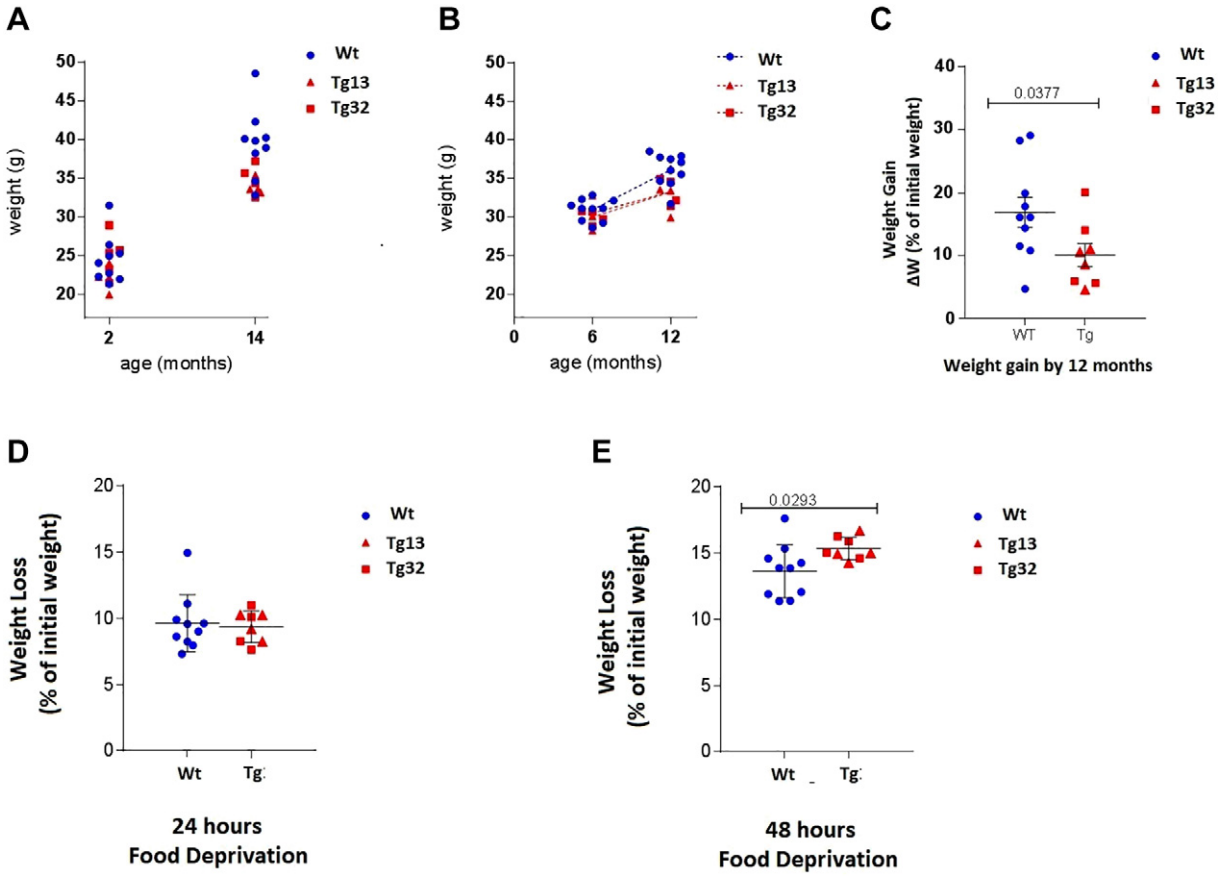

Fig. 6. Effect of aging and food deprivation on body weight balance. A. Comparison of 2-month-old Tg (N = 9) and Wt mice (N = 9) with 14-month-old Tg (N = 9) and Wt (N = 9) mice, reveals that aged animals were significantly heavier than younger mice ($p < 0.001$ for each group). While young adult Tg and Wt mice had a similar body weight, aged Wt mice were significantly heavier that aged Tg mice ($p = 0.0077$). B & C. The body weight of the same Tg or Wt animals was determined at the age of 6 months and then at 12 months. Repeated measures ANOVA revealed a significant genotype effect on body weight changes over time ($p = 0.023$). D & E. Weight loss of Tg and Wt mice following food deprivation. While the two groups lost a comparable amount of weight when deprived of food for 24 h, Tg animals lost significantly more weight than Wt mice after a 48-hour long food deprivation ($p = 0.0293$).

(Fig. 6A). In contrast, aged (14-month-old) Wt mice were significantly heavier (39.5 ± 4.5 g) than aged Tg mice (32.57 ± 1.58 g; $p = 0.0077$) (Fig. 6A). We then followed the animals longitudinally from 6 to 12 months of age and found that, while food consumption was similar in the two groups, Wt mice gained more weight than Tg mice as they grew older (Fig. 6B). Thus, while Wt mice weighed 30.96 ± 1.4 g at 6 months and 36.14 ± 2.09 g at 12 months, Tg mice weighed 30.26 ± 1.40 g at 6 months and 33.30 ± 2.06 g at 12 months (Fig. 6B). As such, Wt and Tg mice were 17 ± 7% and 10 ± 5% heavier, respectively, at 12 months than at 6 months of age (Fig. 6C), suggesting that weight gain was significantly less for Tg than for Wt mice. Analysis of our data with repeated measures ANOVA revealed a significant effect of time on body weight ($p < 0.001$) but also a significant effect of genotype on weight change over time (Wt v/s Tg; $p = 0.023$).

3.8.4. Effect of fasting on body weight

The effect of food deprivation on body weight was also studied. Results revealed that, when deprived of food for 24 h Tg and Wt mice lost a comparable amount of weight (9.4% and 9.6% respectively of their initial weight) (Fig. 6D). However, after 48 hour food deprivation, the Wt mice lost 13.6% and the Tg mice 15.3% of their initial weight ($p = 0.0293$) (Fig. 6E).

4. Discussion

GLUD2 is a primate-specific gene that emerged *via* duplication in the hominoid and evolved on the lineage that descended to the human [3,14]. As such, *GLUD2* is not present in the C57BL/6J mouse strain used here to create our Tg model. Instead, the mouse possesses *Glud1*, the single conserved mammalian gene that is essentially identical to human *GLUD1*. Here we studied hGDH2 expression in the non-neural tissues of Tg mice carrying the human *GLUD2* gene and its regulatory elements. Results showed that hGDH2 is expressed in the adrenals, kidney and testis of the host in a pattern similar to that previously described in human tissues [10]. In the pancreas of Tg mice, hGDH2 was expressed in Langerhans islets, where it localized to insulin-expressing cells of pancreatic islets. In addition, functional studies provided evidence for an enhanced *in vivo* biological action of the novel human enzyme. Specifically, hGDH2 Tg expression "humanized" glucose homeostasis in the host C57BL/6J, a mouse strain prone to diabetes [23]. Thus, while the Wt mice had FBG levels in the pre-diabetic range (136–151 mg/dl), *GLUD2* Tg animals maintained lower FBG levels (91–97 mg/dl) closely resembling those of healthy humans. Also, *GLUD2* exerted a considerable protective effect against the propensity of the host to develop diabetes and to gain weight with advancing age.

To understand the mechanisms by which *GLUD2* transgenic expression affects glucose homeostasis, we determined serum insulin levels before and after administration of glucose or L-leucine, and obtained the following results: Firstly, fasting serum insulin levels were about 2.6-fold higher in the Tg than in the Wt mice. Secondly, in young adult animals, glucose loading produced blood glucose curves and insulin increases, which were comparable in the Tg and Wt mice, thus suggesting that the *GLUD2* gene did not affect glucose-stimulated insulin release. Thirdly, L-leucine loading raised the low insulin levels of the Wt mice, implying a significant activation of the endogenous mGDH1 in β-cells

[12]. These data suggest that L-leucine reached *in vivo*, concentrations sufficient to act synergistically with ADP in counteracting the GTP inhibitory effect on mGDH1 that prevails in β cell [18].

In contrast, L-leucine loading had little effect on Tg mice, which in their fasting state had serum insulin levels higher than those achieved in Wt mice by L-leucine administration. Previous observations have shown that ADP interacts with hGDH2 with higher affinity (SC_{50} = 0.06 mM) than L-leucine (SC_{50} = 1.00 mM) [18] and that 1.00 mM ADP is sufficient to maximally activate hGDH2 [18]. As such, under the low ATP/ADP ratio that prevails in β-cells in the fasting state, glutamate flux through hGDH2 should be close to maximum. Previous studies have indeed showed that ADP attains 1.20 mM at <2.8 mM glucose [24]. Hence, lack of additional L-leucine effect on the high insulin levels of Tg mice support the concept that glutamate flux is close to saturation.

The present studies also revealed that pre-treatment with L-leucine improved glucose handling in both animal groups. Previous investigations on mice with β-cell-specific GDH1 deletion have shown that glutamate deamination *via* GDH1 accounts for about 40% of glucose-stimulated insulin secretion with the enzyme being essential for the full development of the insulin secretory response in β-cells [11]. Hence, the observed improved GTT curves following L-leucine pre-treatment, likely reflect activation of the endogenous mGDH1 possessed by both, the Wt and the Tg mice. Moreover, the stronger L-leucine effect in Tg mice may reflect an additive effect of mGDH1 and hGDH2 in β-cells. Additional studies are required to test this hypothesis and whether hGDH2 and GDH1 form hetero-hexamers with distinct properties in cells co-expressing the two highly homologous isoenzymes.

In recent years, study of mutations in hGDH1 that attenuate GTP inhibition has provided further insight into glutamate-dependent insulin secretory responses [9]. Human subjects, carrying these heterozygous mutations suffer from the HI/HA syndrome, characterized by bouts of hypoglycemia and seizures due to inappropriate release of insulin as a result of an overactive hGDH1 [9]. Similarly, Tg mice, carrying the His454Tyr hGDH1 hyperactive mutant, developed hypoglycemia (blood glucose levels ranging from 50 to 70 mg/dl) that impaired the breeding efficiency and the survival of these animals [25]. These observations have re-enforced the belief that GDH1 in β-cells is largely inactive due to tonic inhibition by GTP generated by the TCA cycle [3].

In contrast to the His454Tyr-hGDH1 Tg mouse, our *GLUD2* Tg mice evidenced no hypoglycemia either during a 6 or 12-hour fasting state or even after L-leucine administration. They also had normal physical health measures, survival and reproduction rates. While hGDH1 mutations result in loss of the physiological hGDH1 regulation, hGDH2 has developed novel molecular mechanisms for regulating its activity as noted above. As such, the beneficial effects of transgenic *GLUD2* expression on glucose homeostasis are likely due to the refined properties acquired by hGDH2 over millions of years of evolution. While these properties include resistance to GTP inhibition (conferred by the Gly456Ala change), the enzyme's functional behavior is multifaceted, being determined by combined actions of other evolutionary amino acid substitutions [15,18]. As a result, *GLUD2* adaptation bestowed human cells with physiologically enhanced glutamate metabolizing capacity that is biologically advantageous.

Regarding the cellular-molecular mechanisms responsible for the observed hGDH2 effects on glucose homeostasis, enzymatic studies, performed *in vitro* using recombinant hGDH1 and hGDH2, have predicted an enhanced *in vivo* biological function for hGDH2 (as compared to hGDH1) in the presence of ADP and L-leucine [3,15,18]. This prediction has been borne out by metabolic studies on cultured human cells expressing hGDH2. Specifically, glioma cells exhibited an enhanced glutamate flux through hGDH2 that non-redundantly increased TCA substrates (α-ketoglutarate, citrate and cis-aconitate) through glutamate oxidation-dependent anaplerosis [26,27]. Similarly, cultured astrocytes isolated from the *GLUD2* Tg mice expressing hGDH2 (constructed independently [28]) exhibited augmented TCA cycle capacity and oxidative metabolism of glutamate, particularly during glucose deprivation [29]. These observations suggested that hGDH2 expression decreased oxidative metabolism of glucose due to increased entrance of carbon skeletons into the TCA from glutamate and other amino acids [29].

In light of the above considerations, augmentation of the bioenergetic and biosynthetic function of the TCA cycle by the expressed hGDH2 in β-cells should account for the observed enhanced insulin secretion in the fasting state. As noted above, hGDH2 should be fully active under the relatively high ADP intracellular concentrations (and low glucose levels) of the fasting state, while mGDH1 is relatively inactive due to tonic inhibition by GTP. Observations in *Glud1* null mice support this concept by showing that absence of mGDH1 in β-cells had no effect on insulin release at 2.8 mM of glucose [11].

While GDH1 is not required for glucose hemostasis under normo-caloric conditions [11], our present data suggest that this role is taken up by the novel positively selected hGDH2 enzyme adapted to function optimally under the high ADP levels of the fasting state. In addition to stimulating hGDH2, the low ATP/ADP ratio of the fasting state increases glutaminolysis (through phosphate-activated glutaminase) [25], thus generating substrate (glutamate) needed for sustaining enhanced oxidative flux through hGDH2. Glutamine is known to be the source of intracellular glutamate and, while glutamine does not promote insulin release, it becomes a secretagogue only when GDH is simultaneously activated [30].

Whereas other mechanisms could play a role on the observed improved glucose homeostasis of Tg mice, we found no significant *GLUD2* expression in non-pancreatic insulin sensitive organs, such as in adipose tissue and skeletal muscle (except for the liver). We also tested here the sensitivity of our animal groups to insulin administration (1 IU/kg body weight, given i.p.). Determination of blood glucose levels every 15 min after insulin administration revealed that glucose levels declined similarly in Wt and Tg mice. These similar insulin tolerance tests for Wt and Tg mice, suggest that the two groups are comparably sensitive to insulin and as such, the high insulin levels of the Tg mice cannot be attributed to a compensatory increased release due to insulin insensitivity. Instead these data support the thesis that hGDH2 expression boosts insulin release through its metabolic function in β-cells (increased ATP synthesis *via* enhanced glutamate oxidation) as described above.

Microscopic examination of the pancreas revealed no changes in the appearance of Langerhans islets, particularly with respect to β-cell mass, density and distribution. Nevertheless, we cannot exclude the possibility that the enhanced basal insulin release could relate to increased overall insulin content in pancreatic β-cell. While additional studies are needed to explore these possibilities, a possible DNA derangement, resulting from stochastic insertion of the human DNA segment into the mouse genome can be essentially excluded as we obtained the same results in two *GLUD2* Tg lines constructed independently.

The present studies also revealed that Wt animals gained more weight than *GLUD2* mice as they grew older. In addition, Wt mice lost less weight than Tg mice following a 48 hour-long food deprivation. Besides the tendency of our C57BL/6J mouse model to develop diabetes, this strain also becomes obese with advancing age [31]. Notably, the *GLUD2* gene attenuated these aging effects, probably by improving cellular energy metabolism. Hence, advent of the *GLUD2* gene may have contributed to the maintenance not only of euglycemia, but also to body weight balance in the human. Whether the novel gene provides protection from disorders of glucose metabolism and obesity associated with senescence is an exciting possibility that remains to be further studied.

Author contributions

CS and AP conceived and coordinated the study and wrote the paper. CS and ZP performed the experimental studies and prepared the Figures. SD and KM contribute to experimental studies. GC designed and

performed the statistical analyses. All authors reviewed the results and approved the final version of the manuscript.

Acknowledgments

We are grateful to Konstantina Aggelaki, Lambros Mathioudakis, Mara Bourbouli and Irene Skoula for their help in these studies.

Declaration of competing interest

The authors declare that they have no conflicts of interest with the contents of this article.

References

[1] Smith EL, Austin BM, Blumenthal KM, Nyc JF. Glutamate dehydrogenase. In: Boyer PD, editor. The enzymes, vol. 11, New York. Academic Press; 1975. p. 293–367.
[2] Mavrothalassitis G, Tzimagiorgis G, Mitsialis A, Zannis V, Plaitakis A, Papamatheakis J, et al. Isolation and characterization of cDNA clones encoding human liver glutamate dehydrogenase: evidence for a small gene family. Proc Natl Acad Sci U S A. 1988;85:3494–8.
[3] Plaitakis A, Kalef-Ezra E, Kotzamani D, Zaganas I, Spanaki C. The glutamate dehydrogenase pathway and its roles in cell and tissue biology in health and disease. Biology (Basel). 2017;6.
[4] Li M, Li C, Allen A, Stanley CA, Smith TJ. The structure and allosteric regulation of mammalian glutamate dehydrogenase. Arch Biochem Biophys. 2012;519:69–80.
[5] Mastorodemos V, Kanavouras K, Sundaram S, Providaki M, Petraki Z, Kokkinidis M, et al. Side-chain interactions in the regulatory domain of human glutamate dehydrogenase determine basal activity and regulation. J Neurochem. 2015;133:73–82.
[6] Spanaki C, Zaganas I, Kounoupa Z, Plaitakis A. The complex regulation of human glud1 and glud2 glutamate dehydrogenases and its implications in nerve tissue biology. Neurochem Int. 2012;61:470–81.
[7] Spanaki C, Kotzamani D, Petraki Z, Drakos E, Plaitakis A. Heterogeneous cellular distribution of glutamate dehydrogenase in brain and in non-neural tissues. Neurochem Res. 2014;39:500–15.
[8] Treberg JR, Banh S, Pandey U, Weihrauch D. Intertissue differences for the role of glutamate dehydrogenase in metabolism. Neurochem Res. 2014;39:516–26.
[9] Stanley CA, Lieu YK, Hsu BY, Burlina AB, Greenberg CR, Hopwood NJ, et al. Hyperinsulinism and hyperammonemia in infants with regulatory mutations of the glutamate dehydrogenase gene. N Engl J Med. 1998;338:1352–7.
[10] Spanaki C, Kotzamani D, Plaitakis A. Widening spectrum of cellular and subcellular expression of human GLUD1 and GLUD2 glutamate dehydrogenases suggests novel functions. Neurochem Res. 2017;42:92–107.
[11] Carobbio S, Frigerio F, Rubi B, Vetterli L, Bloksgaard M, Gjinovci A, et al. Deletion of glutamate dehydrogenase in beta-cells abolishes part of the insulin secretory response not required for glucose homeostasis. J Biol Chem. 2009;284:921–9.
[12] Sener A, Malaisse WJ. L-leucine and a nonmetabolized analogue activate pancreatic islet glutamate dehydrogenase. Nature. 1980;288:187–9.
[13] Shashidharan P, Michaelidis TM, Robakis NK, Kresovali A, Papamatheakis J, Plaitakis A. Novel human glutamate dehydrogenase expressed in neural and testicular tissues and encoded by an X-linked intronless gene. J Biol Chem. 1994;269:16971–6.
[14] Burki F, Kaessmann H. Birth and adaptive evolution of a hominoid gene that supports high neurotransmitter flux. Nat Genet. 2004;36:1061–3.
[15] Plaitakis A, Latsoudis H, Spanaki C. The human GLUD2 glutamate dehydrogenase and its regulation in health and disease. Neurochem Int. 2011;59:495–509.
[16] Zaganas I, Plaitakis A. Single amino acid substitution (G456A) in the vicinity of the GTP binding domain of human housekeeping glutamate dehydrogenase markedly attenuates GTP inhibition and abolishes the cooperative behavior of the enzyme. J Biol Chem. 2002;277:26422–8.
[17] Zaganas I, Spanaki C, Karpusas M, Plaitakis A. Substitution of Ser for Arg-443 in the regulatory domain of human housekeeping (GLUD1) glutamate dehydrogenase virtually abolishes basal activity and markedly alters the activation of the enzyme by ADP and L-leucine. J Biol Chem. 2002;277:46552–8.
[18] Kanavouras K, Mastorodemos V, Borompokas N, Spanaki C, Plaitakis A. Properties and molecular evolution of human GLUD2 (neural and testicular tissue-specific) glutamate dehydrogenase. J Neurosci Res. 2007;85:3398–406.
[19] Shashidharan P, Clarke DD, Ahmed N, Moschonas N, Plaitakis A. Nerve tissue-specific human glutamate dehydrogenase that is thermolabile and highly regulated by ADP. J Neurochem. 1997;68:1804–11.
[20] Plaitakis A, Kotzamani D, Petraki Z, Delidaki M, Rinotas V, Zaganas I, et al. Transgenic mice carrying GLUD2 as a tool for studying the expressional and the functional adaptation of this positive selected gene in human brain evolution. Neurochem Res. 2019;44:154–69.
[21] Spanaki C, Plaitakis A. The role of glutamate dehydrogenase in mammalian ammonia metabolism. Neurotox Res. 2012;21:117–27.
[22] Spanaki C, Kotzamani D, Petraki Z, Drakos E, Plaitakis A. Expression of human GLUD1 and GLUD2 glutamate dehydrogenases in steroid producing tissues. Mol Cell Endocrinol. 2015;415:1–11.
[23] Ayala JE, Samuel VT, Morton GJ, Obici S, Croniger CM, Shulman GI, et al. Standard operating procedures for describing and performing metabolic tests of glucose homeostasis in mice. Dis Model Mech. 2010;3:525–34.
[24] Detimary P, Dejonghe S, Ling Z, Pipeleers D, Schuit F, Henquin JC. The changes in adenine nucleotides measured in glucose-stimulated rodent islets occur in beta cells but not in alpha cells and are also observed in human islets. J Biol Chem. 1998;273:33905–8.
[25] Li C, Matter A, Kelly A, Petty TJ, Najafi H, MacMullen C, et al. Effects of a GTP-insensitive mutation of glutamate dehydrogenase on insulin secretion in transgenic mice. J Biol Chem. 2006;281:15064–72.
[26] Chen R, Nishimura MC, Kharbanda S, Peale F, Deng Y, Daemen A, et al. Hominoid-specific enzyme GLUD2 promotes growth of IDH1R132H glioma. Proc Natl Acad Sci U S A. 2014;111:14217–22.
[27] Waitkus MS, Pirozzi CJ, Moure CJ, Diplas BH, Hansen LJ, Carpenter AB, et al. Adaptive evolution of the GDH2 allosteric domain promotes gliomagenesis by resolving IDH1 (R132H)-induced metabolic liabilities. Cancer Res. 2018;78(1):36–50.
[28] Li Q, Guo S, Jiang X, Bryk J, Naumann R, Enard W, et al. Mice carrying a human GLUD2 gene recapitulate aspects of human transcriptome and metabolome development. Proc Natl Acad Sci U S A. 2016;113:5358–63.
[29] Nissen JD, Lykke K, Bryk J, Stridh MH, Zaganas I, Skytt DM, et al. Expression of the human isoform of glutamate dehydrogenase, hGDH2, augments TCA cycle capacity and oxidative metabolism of glutamate during glucose deprivation in astrocytes. Glia. 2017;65:474–88.
[30] Vetterli L, Carobbio S, Pournourmohammadi S, Martin-Del-Rio R, Skytt DM, Waagepetersen HS, et al. Delineation of glutamate pathways and secretory responses in pancreatic islets with beta-cell-specific abrogation of the glutamate dehydrogenase. Mol Biol Cell. 2012;23:3851–62.
[31] The Jackson Laboratory. C57BL/6J mouse strain data sheet. . https://www.jax.org/strain/000664. Accessed date: 19 March 2019.